CrossMark

Comprehensive Study of the Blazars from Fermi-LAT LCR: The Log-Normal Flux Distribution and Linear rms–Flux Relation

Na Wang[1,2,3], Ting-Feng Yi[1,2,3], Liang Wang[1], Li-Sheng Mao[1], Zhi-Yuan Pu[1], Gong-Ming Ning[1], Wei-Tian Huang[1], He Lu[1],
Shun Zhang[1], Yu-Tong Chen[1], and Liang Dong[3]
[1] Department of Physics, Yunnan Normal University, Kunming 650500, China; yitingfeng@ynnu.edu.cn
[2] Guangxi Key Laboratory for the Relativistic Astrophysics, Nanning 530004, China
[3] Yunnan Province China-Malaysia HF-VHF Advanced Radio Astronomy Technology International Joint Laboratory, Kunming 650011, China

Abstract

Fermi-LAT LCR provides continuous and regularly sampled gamma-ray light curves, spanning about 14 yr, for a large sample of blazars. The log-normal flux distribution and linear rms–flux relation of the light curves for a few Fermi blazars have been examined in previous studies. However, the probability that blazars exhibit the log-normal flux distribution and linear rms–flux relation in their gamma-ray light curves has not been systematically explored. In this study, we comprehensively research the distribution of γ-ray flux and the statistical characteristics on a large sample of 1414 variable blazars from the Fermi-LAT LCR catalog, including 572 FSRQs, 477 BL Lacs, and 365 BCUs, and statistically compare their flux distributions with normal and log-normal distributions. The results indicate that the probability of not rejecting log-normal is 42.05% for the large sample, and there is still a 2.05% probability of not rejecting normality, based on the joint of Kolmogorov–Smirnov, Shapiro–Wilk, and Normality tests. We further find that the probability that BL Lacs conform to the log-normal distribution is higher than that of FSRQs. Besides, after removing sources with less than 200 data points from this large sample, a sample of 549 blazars, which is still a large sample compared to the previous studies, was obtained. Based on dividing the light curves into segments every 20 points (or 40 points, or one year), we fitted the linear rms–flux relation of these three different sets and found that the Pearson correlation coefficients are all close to 1 for most blazars. This result indicates a strong linear correlation between the rms and the flux of these 549 blazars. The log-normal distribution and linear rms–flux relation indicate that the variability of the γ-ray flux for most blazars is a non-linear and multiplicative process.

Key words: (galaxies:) quasars: general – (galaxies:) BL Lacertae objects: general – galaxies: jets – galaxies: active

1. Introduction

Blazars, a special subclass of Active Galactic Nuclei (AGNs), exhibit unique properties that are notably characterized by their highly relativistic jets which are oriented in the direction of the line of sight of the observers (Urry & Padovani 1995; Jovanović et al. 2023). These objects exhibit extreme observational properties including high luminosity, high polarization, and fast variability. Blazars are divided into two sub-classes: BL Lac objects (BL Lacs) and Flat-Spectrum Radio Quasars (FSRQs). The spectra of BL Lacs have only faint emission lines or no emission lines, but FSRQs have strong emission lines (Urry & Padovani 1995; Abdo et al. 2010). In the past thirty years, with the development of gamma-ray astronomy, it has become possible to study the temporal and spectral behavior of blazars in detail. The Fermi telescope provided a platform for exploring high-energy γ-ray sources outside the Galaxy (Atwood et al. 2009; Razzano et al. 2009). The latest catalog update includes over 5000 γ-ray sources above 4σ significance, 60% of which are blazars (Abdollahi et al. 2020).

The flux distribution of blazars has been studied in many literatures to understand the nature of emission processes (Urry & Padovani 1995; Biteau & Giebels 2012a; Bhatta & Dhital 2020; Khatoon et al. 2020). A number of blazars observed by Fermi-LAT show log-normal distribution in their long-term γ-ray light curves (Scarpa & Falomo 1997; Uttley et al. 2005; Ackermann et al. 2015; Romoli et al. 2018; Shah et al. 2018; Bhatta & Dhital 2020; Zhang et al. 2022, 2023). In recent years, the progress of astronomical observations has provided important conditions for analyzing long-term flux distributions. The multiple investigations have yielded log-normal distributions of X-ray flux existing in AGNs, and X-ray binaries (Lyubarskii 1997; Uttley & McHardy 2001; Quilligan et al. 2002; McHardy 2010). Subsequently, a log-normal distribution of flux was discerned in the γ-ray light curves of PKS 1510-089 and PKS 2155-304, with a linear correlation

linking the root mean square (rms) and the average flux (Kushwaha et al. 2016; H.E.S.S. Collaboration et al. 2017).

Lyutyj & Oknyanskij (1987) find that the linear correlation between X-ray flux and its corresponding variation implies a log-normal distribution in the Seyfert galaxy. In the X-ray band, many AGNs exhibit both log-normal distribution and the rms–flux linear connection (McHardy et al. 2004; Kushwaha et al. 2017). The proportional linear correlation denoted that the absolute amplitude of rms and mean flux were linked, thereby inferring that sources with greater luminosity evince greater degrees of rms fluctuation. Furthermore, this linear relationship may possess a more intrinsic and fundamental than the PSD (Power Spectral Density) (McClintock et al. 2003; Gleissner et al. 2004; Pottschmidt et al. 2004). It has always been controversial that the flux variability of blazars originated from the jet itself or the disk that could modulate the jet emission. The rms–flux linear connection can promote the study of potential physical process changes in blazars. Therefore, the linear rms–flux relation is of great significance for the time variable analysis of the blazars, and it is helpful for us to understand the origin of the variability of blazars.

In the γ-ray band, this rms–flux relation and log-normal distribution was researched for some individual sources, such as Mrk 421, Mrk 501, 1ES 1011+496 (Tluczykont et al. 2010; Chakraborty et al. 2015; Sinha et al. 2017). A small sample of log-normal distribution was also investigated (Kushwaha et al. 2017; Shah et al. 2018; Bhatta & Dhital 2020). However, there is still a lack of systematic research on flux distribution and rms–flux relation of the γ-ray of blazars. In order to further systematically study the rms–flux relation and the flux distribution of the blazars. We will perform a comprehensive study on the γ-ray flux of the Fermi-LAT blazars, based on a large sample. From the 1525 variable sources (variable index more than 21.67) of the Fermi-LAT LCR catalog (Abdollahi et al. 2023), we obtained a large sample including 1414 variable blazars. They have been continuously monitored at a cadence of three days, making them well-suited for time series analysis. The data samples are described in Section 2. The flux distributions are fitted by both the normal and log-normal functions in Section 3. In Section 4, we analyze and fit the rms–flux relation on the light curve by using three different binnings, and compare results statistically between the three subtypes of sources, FSRQs, BL Lacs, and blazar candidate of uncertain types (BCUs). The results and possible implications are discussed in Section 5.

2. Data Samples

In 2008, the Fermi Gamma-ray Space Telescope was launched with the Large Area Telescope (LAT) as the principal tool in its scientific repertoire. It usually runs in scan mode and covers the entire γ-ray photon events in the sky range from 20 MeV to >300 GeV every ∼3 hr with a field of view of ∼2.4

steradian. The telescope provides continuous and nearly uniform observations of persistent and transient γ-ray sources with the longest and most uniformly sampled γ-ray data (Abdo et al. 2009). The light curves on time intervals of 30 days (monthly), 7 days (weekly), and 3 days for 1414 variable blazar sources (variable index more than 21.67) in the Fermi-LAT LCR (Abdollahi et al. 2023). Here, the light curves on the cadence of 3 days with minimum detection significance TS > 4 (2σ) from 2008 to now are chosen providing more data points for studying the rms–flux relation and flux distribution. We further investigated or removed any outliers (photon flux $>5 \times 10^{-5}$) before using the data for detailed analysis. These blazars can be classified into FSRQs, BL Lacs, and BCUs, accounting for 40.453%, 33.734%, and 25.813% of the samples respectively. We use the light curves of the blazars of these three types to study the flux distribution. After removing sources with less than 200 data points (to reduce the influence to rms–flux from the small number of data points in per bin) from this large sample, we obtain a subsample including 41 BCUs, 236 BL Lacs, and 272 FSRQs for fitting rms–flux relation.

3. Flux Distribution Analysis

Histograms are a valuable tool for characterizing the flux distribution of blazars. The flux histograms of 365 BCUs, 477 BL Lacs, and 572 FSRQs are shown in Figure 1. We find that most histograms have a prominent peak and a high flux tail. To further understand the distributions, we fit them with normal and log-normal functions and compared the results using reduced χ^2. The fit parameters together with the reduced χ^2 for both distributions are shown in Table 1. We also compare the results by three tests, including the Kolmogorov–Smirnov (K-S), the Shapiro–Wilk (S-W), and the Normality tests in Table 1. We conducted statistical analysis on the results of three tests and reduced χ^2 for BCUs, BL Lacs, and FSRQs.

We count the proportion of FSRQs, BL Lacs, and BCUs in Table 1 that did not reject the null hypothesis under the three tests of K-S, S-W, and Normality tests, i.e., the proportion of p-values. As shown in Table 2, statistical analysis results of three tests are computed about 572 FSRQs to verify the normality or lognormality of the probability density function (PDF) from these histograms. Out of the three tests, the percentages that do not reject normal distribution are 20.98%, 1.92%, and 2.45%, respectively ($p > 0.05$). On the other hand, the percentages of FSRQs that do not reject the log-normal distribution of flux are 77.45%, 37.41%, and 37.41%, respectively. Among the 477 selected BL Lacs, as shown in Table 2, we perform a similar analysis process as for FSRQs. The percentages of BL Lacs that do not reject normal distribution are 21.59%, 0.84%, and 1.89%, while 95.18%, 52.41%, and 52.83% of BL Lacs do not reject log-normal of the flux distribution, respectively. Apart from FSRQs and BL Lacs, there are 365 BCUs that lack
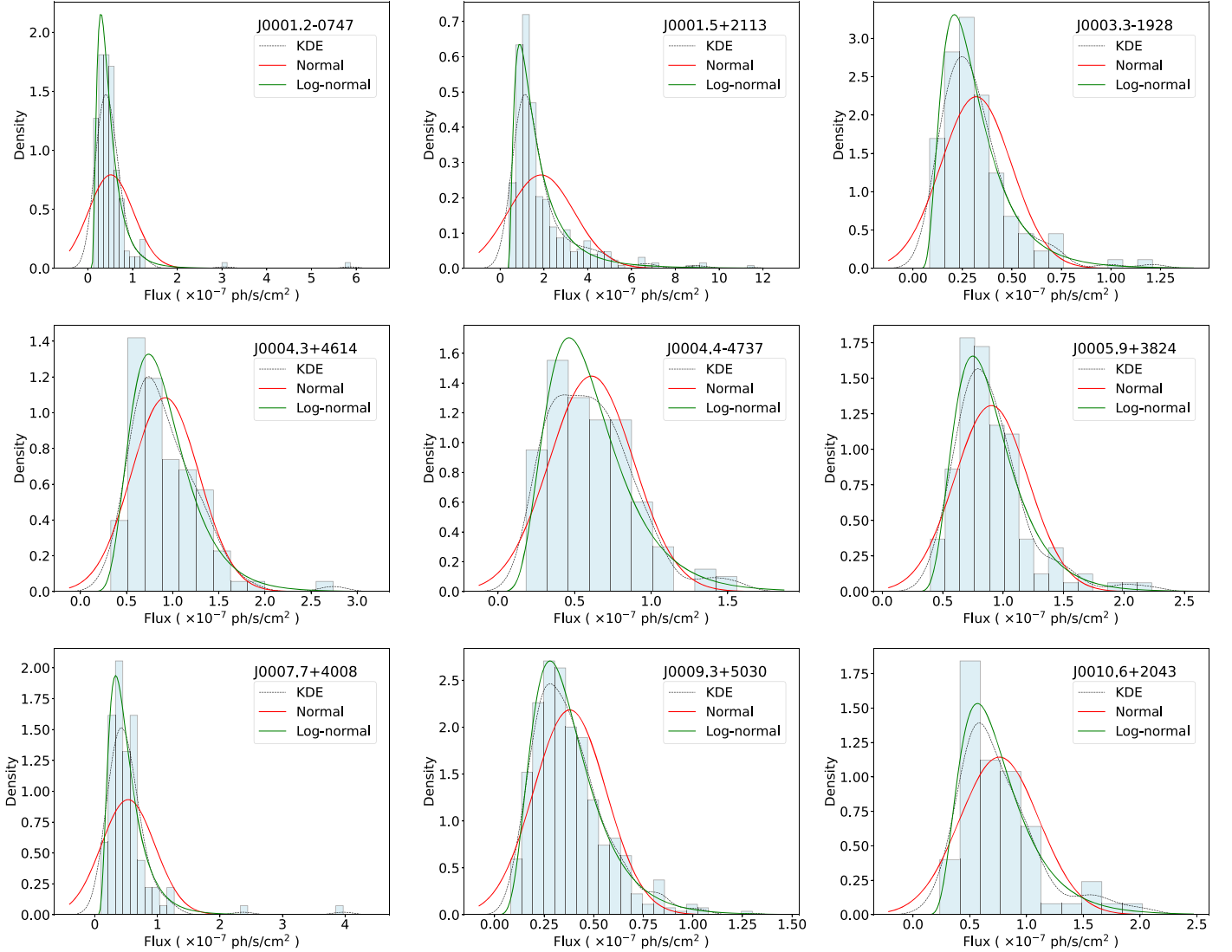
Figure 1. The normal (red solid line) and log-normal (green solid line) function fitting to the γ-ray flux distribution (hatched blue histogram) of the blazars, the black dotted line represents the kernel density estimation (KDE) curve. Here, the figure lists only the first nine sources. The entire figure is available in its entirety in machine-readable form.

reliable classification. To study the flux distribution characteristics of these 365 BCUs, we also analyze them as described above, and the results of the analysis are shown in Table 2. For the three different tests, we find that there are differences in the results of the three tests, among which the results of the K-S test are significantly different from the results of the S-W test and the Normality test, and the results of the S-W test and the Normality test are basically the same. In order to unify the results, we define the flux distribution of blazars that do not reject the null hypothesis under all three tests as distributions that consist of the null hypothesis. Under this standard, out of 1414 variable blazars, flux distribution for 199 FSRQs, 230 BL Lacs, and 179 BCUs consists of the log-normal distribution.

However, of these 1414 variable blazars, the flux distribution of 9 FSRQs, 4 BL Lacs, and 16 BCUs, respectively, conform to the normal distribution.

Furthermore, based on the K-S, S-W, and Normality test results, the distribution of p-values was obtained. As shown in Figure 2, the p-value distributions of the FSRQs, BL Lacs, and BCUs are similar. These distributions reveal that the p-values of the K-S (Log-normal), S-W (Log-normal), and Normality (Log-normal) tests are predominantly concentrated in the range where $p > 0.05$. Conversely, p-values of the three tests (Normal) are mainly concentrated in the range where $p < 0.05$. Generally, the more the flux distribution of blazars in the sample fits the Log-normal distribution, the less flux

Table 1
Parameters of Log-normal and Normal Distribution Fitting for the γ-Ray Flux Distribution of the Fermi-LAT Sources

Name(type)	Log-normal Fit						Normal Fit					
	Mean	σ	K-S Test(prob)	S-W Test(prob)	Normlity (prob)	Reduced χ^2	Mean	σ	K-S Test(prob)	S-W Test(prob)	Normlity (prob)	Reduced χ^2
J0001.2-0747(bll)	-0.85	0.55	4.78×10^{-1}	7.44×10^{-5}	3.34×10^{-7}	35.53	0.51	0.50	8.79×10^{-9}	2.11×10^{-23}	1.23×10^{-63}	>100
J0001.5+2113(fsrq)	0.41	0.62	1.64×10^{-3}	4.35×10^{-9}	2.70×10^{-7}	6.92	1.87	1.51	7.78×10^{-16}	1.45×10^{-25}	1.00×10^{-54}	>100
J0003.3-1928(fsrq)	-1.27	0.50	9.21×10^{-1}	9.65×10^{-1}	7.49×10^{-1}	0.79	0.32	0.18	7.99×10^{-3}	1.36×10^{-9}	3.67×10^{-14}	>100
J0004.3+4614(fsrq)	-0.16	0.38	9.41×10^{-1}	6.15×10^{-1}	6.82×10^{-1}	0.87	0.92	0.37	2.53×10^{-1}	2.03×10^{-6}	3.76×10^{-10}	>100
J0004.4-4737(fsrq)	-0.60	0.46	5.30×10^{-1}	1.50×10^{-1}	2.28×10^{-1}	1.42	0.61	0.28	4.26×10^{-1}	1.35×10^{-5}	2.80×10^{-5}	4.90
J0005.9+3824(bcu)	-0.15	0.31	8.42×10^{-1}	1.81×10^{-1}	5.71×10^{-2}	1.96	0.90	0.31	5.14×10^{-2}	1.09×10^{-8}	4.60×10^{-12}	44.77
J0007.7+4008(bll)	-0.79	0.54	3.66×10^{-1}	7.70×10^{-3}	7.43×10^{-4}	3.19	0.53	0.43	9.53×10^{-6}	4.70×10^{-17}	4.99×10^{-36}	>100
J0009.3+5030(bll)	-1.08	0.48	8.28×10^{-1}	5.06×10^{-1}	3.51×10^{-1}	0.74	0.38	0.18	7.46×10^{-4}	7.65×10^{-15}	2.14×10^{-23}	50.41
J0010.6+2043(bll)	-0.36	0.42	3.80×10^{-1}	2.50×10^{-1}	4.95×10^{-1}	1.47	0.76	0.35	4.01×10^{-2}	2.70×10^{-6}	1.89×10^{-6}	5.41

Note. The table lists only the first nine blazars.

distribution of blazars fits the normal distribution. These consistent results indicate that the flux distributions of the three subtypes of blazars prefer log-normal distribution over normal distribution.

The results in Table 2 and Figure 2 of the three tests indicate that most of the blazars prefer log-normal distribution. According to the comparison of flux distribution from three test results, the probability that BL Lacs consist with the log-normal distribution is higher than that of FSRQs, while the probability that BCUs conform to the log-normal distribution is similar to that of BL Lacs. The histograms and fits are shown in Figure 1.

In the multiplicative model, the flux naturally generates a log-normal distribution. If we let ϕ be the product of flux A in a large number of isotropic regions that is,

$$\phi = \prod_{i=1}^{n} (A_n) \qquad (1)$$

$$\log(\phi) = \log\left(\prod_{i=1}^{n} (A_n) \right) \qquad (2)$$

$$\log(\phi) = \sum_{i=1}^{n} \log(A_n) \qquad (3)$$

Then $\log\phi$ is the sum of $\log A$. Pursuant to the Central Limit Theorem (CLT), it can be adduced that the logarithmic value of ϕ ensues a normal distribution, or in other words, ϕ adheres to a distribution that is log-normal (Biteau & Giebels 2012b). Assuming in the context of a log-normal distribution, the observed flux ϕ can be expressed as a function of an underlying variable x, that is, $\phi = f(x)$. In this distribution, the function f follows an exponential pattern while the variable x conforms to a normal distribution. Fluctuations in x in the form of a slight deviation from a given value, namely δx, result in corresponding deviations in ϕ around $f(x_0)$, $\delta\phi$ (Biteau & Giebels 2012a). It is noteworthy that the flux's variance is

Table 2
The Statistical Results of Normal and Log-normal Flux Distribution of Three Subtypes of Blazars

FSRQs		
Type of Test	Fraction of not Reject Normal ($p > 0.05$)	Fraction of not Reject log-normal ($p > 0.05$)
K-S test	20.98%	77.45%
S-W test	1.92%	37.41%
Normality test	2.45%	37.41%
joint of the three tests	1.57%	34.79%
BL Lacs		
K-S test	21.59%	95.18%
S-W test	0.84%	52.41%
Normality test	1.89%	52.83%
joint of the three tests	0.84%	48.22%
BCUs		
K-S test	43.01%	92.60%
S-W test	4.93%	53.97%
Normality test	6.03%	53.15%
joint of the three tests	4.38%	49.04

inexorably dependent on that of the variable x, and the variance of the flux is

$$\delta\phi^2 = \left[\frac{\partial f}{\partial x}(x_0) \right]^2 \delta x^2. \qquad (4)$$

When the flux deviation is proportional to $f(x_0)$, the relation can be equivalent to

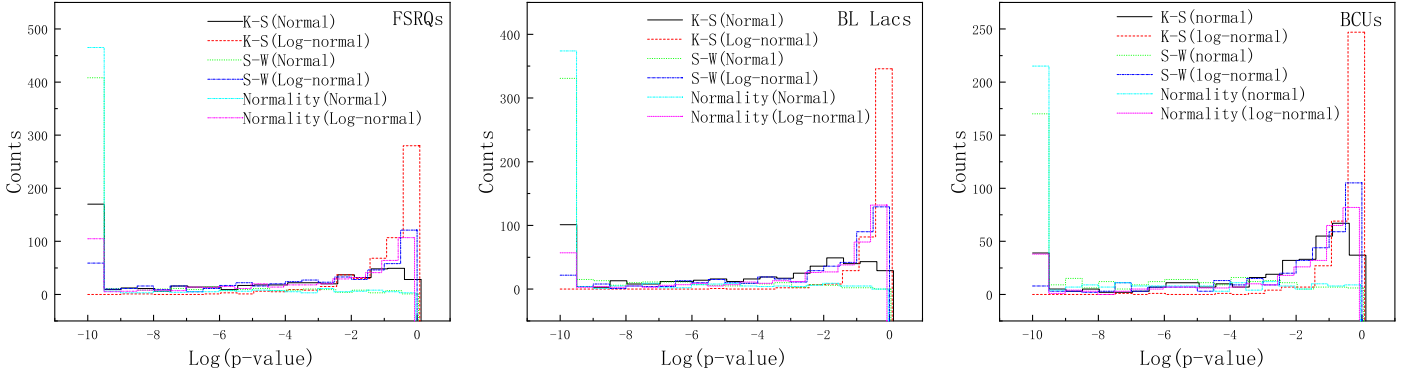$$f(x_o)^2 \propto \left[\frac{\partial f}{\partial x}(x_0) \right]^2 \delta x^2. \qquad (5)$$

Figure 2. Distributions of *p*-value of K-S, S-W, and Normality tests for lognormality and normality of the flux distribution from blazars, respectively. The left, center, and right panels represent the statistical results for FSRQs, BL Lacs, and BCUs, respectively.

This equation is one of the definitions of the exponential function. The flux is proportional to its rms only when the flux is an exponent of the underlying variable. Therefore, the rms–flux relation can be interpreted as a consequence of a log-normal distribution of the flux (Uttley et al. 2005; Biteau & Giebels 2012a, 2012b).

4. Rms–Flux Relation

The rms–flux relation has been most convincingly demonstrated on relatively short timescales in the X-ray band. In order to study rms–flux relations of blazars in the γ-ray band, the 1414 blazars are chosen from Fermi-LAT LCR. In order to avoid the too small number of bins that will affect the statistical significance of fitting results, we choose blazars with data points greater than 200 as a subsample. After removing sources with less than 200 data points from this large sample, we obtained a sample including 41 BCUs, 236 BL Lacs, and 272 FSRQs. We separately fit and estimate the rms–flux relation for three different binnings of light curves: 20 data points, 40 data points, and one year (365 days) per bin, and calculate their Pearson correlation coefficients. These three kinds of binnings are based on time series. The first two binnings involve dividing the data point into bin of fixed point numbers, with each bin consisting of 20 data points and 40 data points, respectively. In order to further investigate whether the binnings have an impact on the rms–flux relation, the third binnings involves grouping the data based on fixed time intervals, with all points within 365 days (yearly) interval forming a bin. We calculate the rms and average flux for each bin and perform a linear regression analysis. Therefore, we obtain the Pearson correlation coefficient for the rms–flux. We can see that the interdependence between rms and flux is noteworthy, with a substantial and coherent correlation between the two. Linear fitted plots of rms–flux relation are shown in Figure 3.

Statistical results of three different binnings are shown in Figure 4 and Table 3. As shown in Table 4, when 20 data

points are taken as a bin, the mean slope of the rms–flux for FSRQs, BL Lacs, and BCUs are 1.860, 1.996, and 1.985, respectively. The mean Pearson correlation coefficients for rms–flux relation for all three types are 0.977, 0.961, and 0.979, respectively. Thus, there is a strong correlation between rms and flux. For the other two binnings, the Pearson correlation coefficients for rms–flux are ∼1, indicating a strong linear rms–flux relation for all 549 sources, as shown in Table 4.

Based on the fitting of the rms–flux relation for BL Lacs, FSRQs, and BCUs using different grouping schemes, the slopes for these three types of sources are greater than zero. The BL Lacs exhibit a steeper slope in relation to the FSRQs. However, the differences in slopes obtained from the three types of sources are too small, therefore the slope cannot be used as a criterion to distinguish between the three source types.

5. Discussion and Conclusion

In this work, we investigate the variability properties of the γ-ray by analyzing the flux distribution and the linear rms–flux relation of a large blazar sample from Fermi-LAT LCR, including 572 FSRQs, 477 BL Lacs, and 365 BCUs. We fitted the flux distribution histograms to determine whether the flux distribution conforms to normal or log-normal functions. Of the 572 FSRQs, 199 FSRQs consist of a log-normal distribution for flux and only 9 FSRQs follow a normal distribution. Of the 477 BL Lacs, 230 BL Lacs consist of a log-normal distribution and only four BL Lacs follow a normal distribution. In the case of 365 BCUs, there are 179 BCUs consisting of log-normal distribution of flux and only five BCUs consist of normal. The probability that the flux distribution of BL Lacs shows log-normal is greater than that of FSRQs. Interestingly, we find that the flux of a few sources is normally distributed, and the flux distribution is also consistent with log-normal distribution. Further analysis is required for those blazars whose distribution does not conform to either the log-normal distribution or the normal distribution. In particular, the S5 0716+714 γ-ray flux
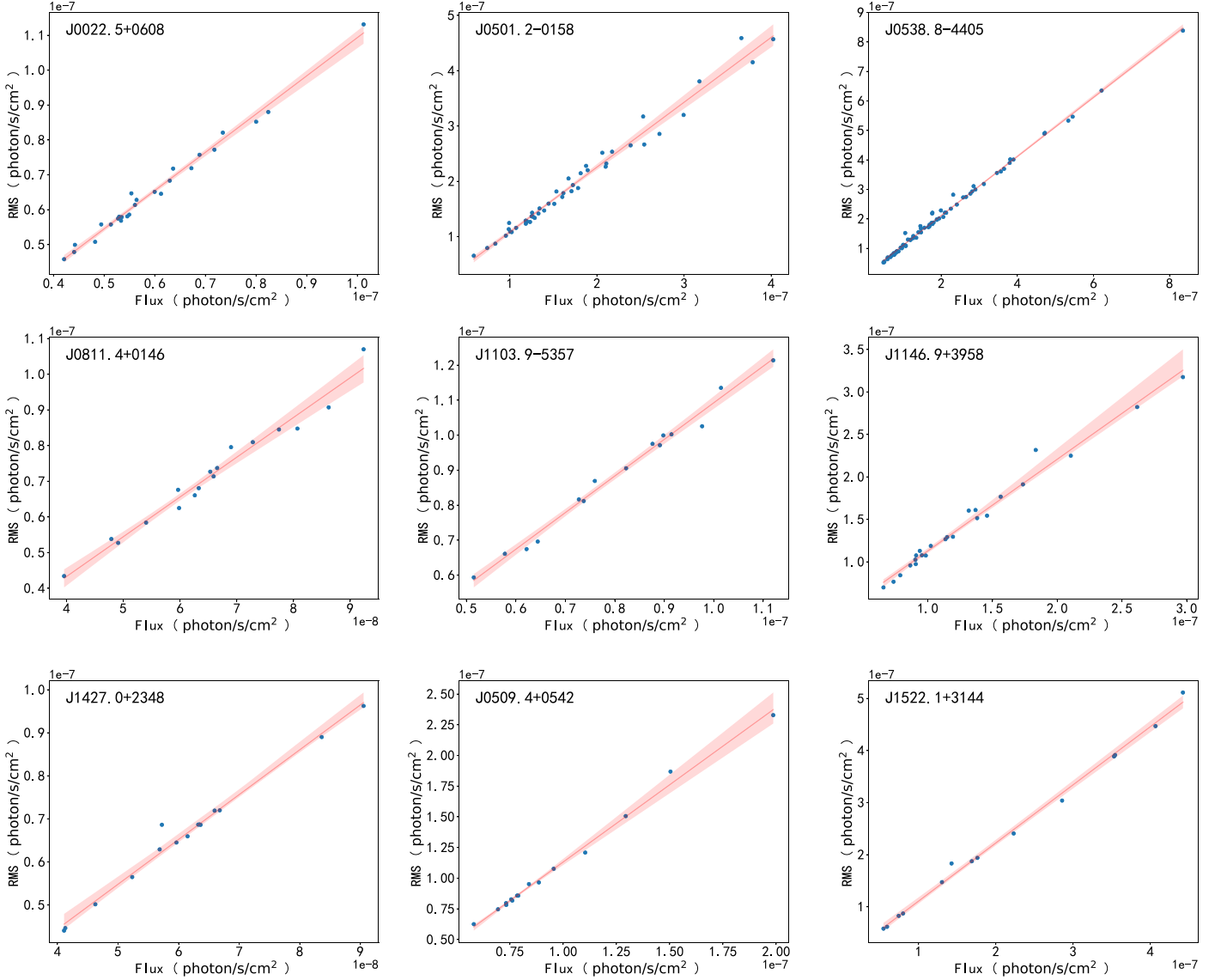
Figure 3. Graphs of rms–flux relation of three randomly selected sources for each binning. The first row is the 20 data points per bin for rms–flux relation. The second row is the 40 data points per bin for rms–flux relation. The third row is the 365 days per bin for rms–flux relation. The figure lists only the first nine sources.

distribution with both normal and log-normal PDF was fitted, and found that the normal PDF fitted light curves (28 days binnings) best (Peñil et al. 2022). However, for the same source, our fit to the flux distribution follows a log-normal distribution (3 days binnings). Peñil et al. (2022) used 28-day binning for the light curves, while we used 3 day binned light curves. This indicates binning for light curves will affect the fitting results. As shown in Figure 5, we also found some histograms showing bimodal patterns, and the statistics of this distribution are not significant enough, hence these results should be taken only as indicative. In addition to using Fermi data with TS > 4, we try to use the Fermi data with TS > 9 to study flux distribution and summarize the results under the

K-S, S-W, and Normality tests. We conduct statistical analysis on the data of the three test results. For the K-S test, 86.21% of the blazars of flux distributions have a log-normal distribution, while 57.99% of the blazars of flux distributions show a normal distribution. In the S-W test, 61.60% of the blazars of flux distributions have a log-normal distribution, while 24.47% of the blazars of flux distributions show a normal distribution. For the Normality test, 60.82% of the blazars of flux distributions have a log-normal distribution, while 28.08% of the blazars of flux distributions show a normal distribution. The flux distribution also generally tends to be log-normal. The number of data points with TS > 9 per bins is too small which will affect the statistical significance of fitting results. So we have
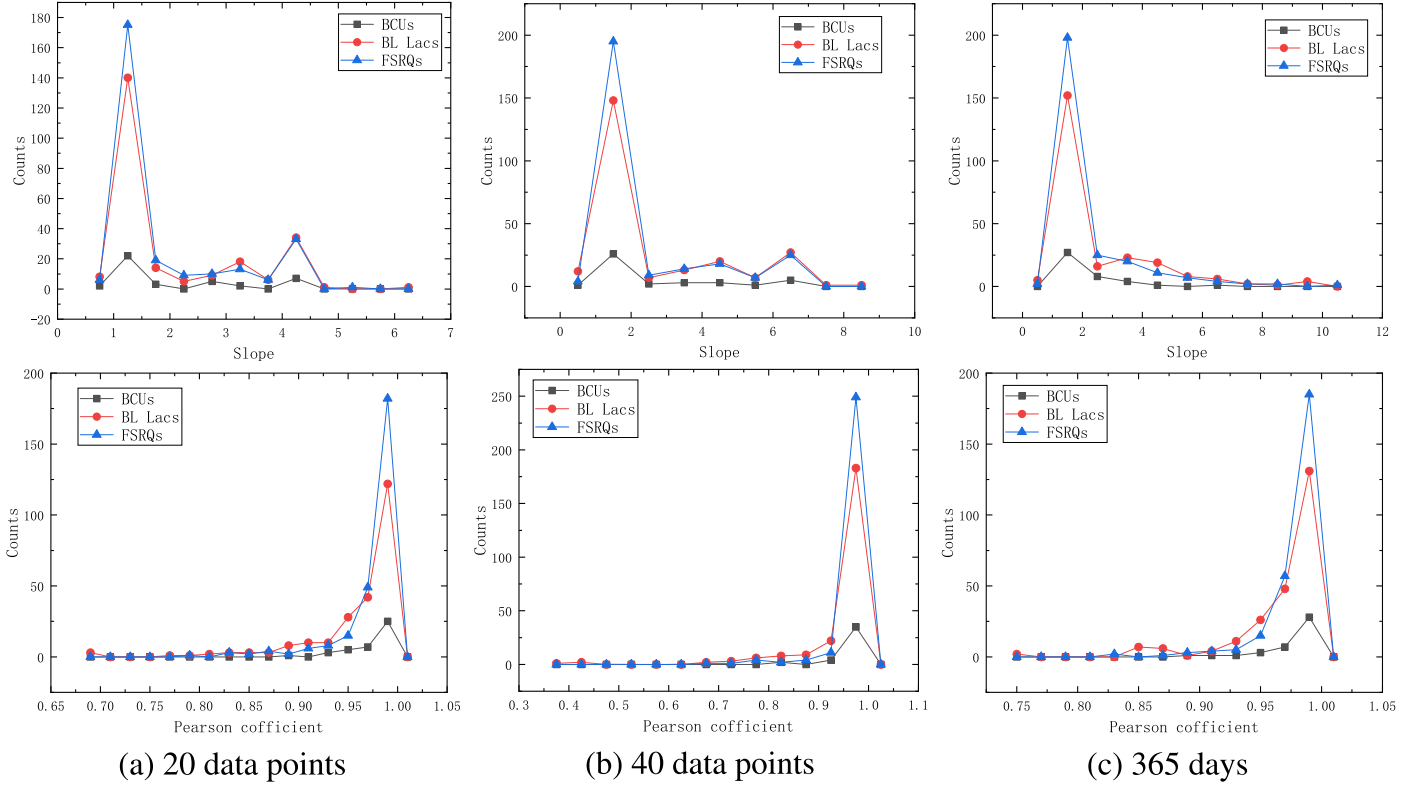
Figure 4. Statistical results for three different binnings, including 20 data points, 40 data points, and 365 days, according to column a, b, c, respectively. The first row is the distribution of slope for three binnings. The second row is the distribution of Pearson correlation coefficients.

Table 3
Statistical Results for Three Different Binnings, Including 20 Data Points, 40 Data Points and 365 days

Name(type)	20 Data Points Bin			40 Data Points Bin			365 days		
	Slope	Intercept	Pearson Correlation	Slope	Intercept	Pearson Correlation	Slope	Intercept	Pearson Correlation
J0001.5+2113(fsrq)	1.267	-1.983×10^{-8}	0.987	1.246	-1.027×10^{-8}	0.988	1.433	-4.117×10^{-8}	0.994
J0009.3+5030(bll)	4.363	-1.276×10^{-7}	1.000	6.247	-2.037×10^{-7}	1.000	4.675	7.123×10^{-8}	0.990
J0011.4+0057(fsrq)	1.357	-1.514×10^{-8}	0.961	1.298	-6.288×10^{-9}	0.991	1.143	9.950×10^{-9}	0.941
J0017.5-0514(fsrq)	1.462	-2.569×10^{-8}	0.786	1.649	-5.104×10^{-8}	0.957	1.434	-3.059×10^{-8}	0.964
J0019.6+7327(fsrq)	1.390	-4.960×10^{-8}	0.962	1.304	-3.301×10^{-8}	0.977	1.345	-4.573×10^{-8}	0.985
J0022.5+0608(bll)	1.096	-2.997×10^{-10}	0.994	1.076	1.207×10^{-9}	0.995	1.005	5.024×10^{-9}	0.980
J0028.4+2001(fsrq)	1.040	1.328×10^{-8}	0.997	1.038	2.068×10^{-8}	0.998	1.263	-1.431×10^{-8}	0.998
J0030.3-4224(fsrq)	1.432	-2.576×10^{-8}	0.980	1.651	-4.226×10^{-8}	0.978	1.164	2.797×10^{-9}	0.894
J0030.6-0212(bcu)	1.159	-1.776×10^{-9}	0.983	1.146	-4.479×10^{-10}	0.991	1.326	-1.904×10^{-8}	0.995

Note. The table lists only the first nine blazars.

not analyzed the rms–flux relationship of the the data with TS > 9.

There are many literatures that explain why the log-normal distribution is in many sources and in different bands (Kirk et al. 1998; Giebels & Degrange 2009; Kushwaha et al. 2017; Shah et al. 2018, 2020; Khatoon et al. 2020; Scargle 2020). The variability of the blazars may be due to a combination of

intrinsic events of the source, such as instability of both the disk and the jet, and extrinsic influences on the source's geometry and projection. For instance, there are mainly three explanatory models for the log-normal distribution: (1) In the X-ray band, it was initially believed that the log-normal distribution of the flux was from accretion disks, the propagating fluctuations model proposed by Lyubarskii to
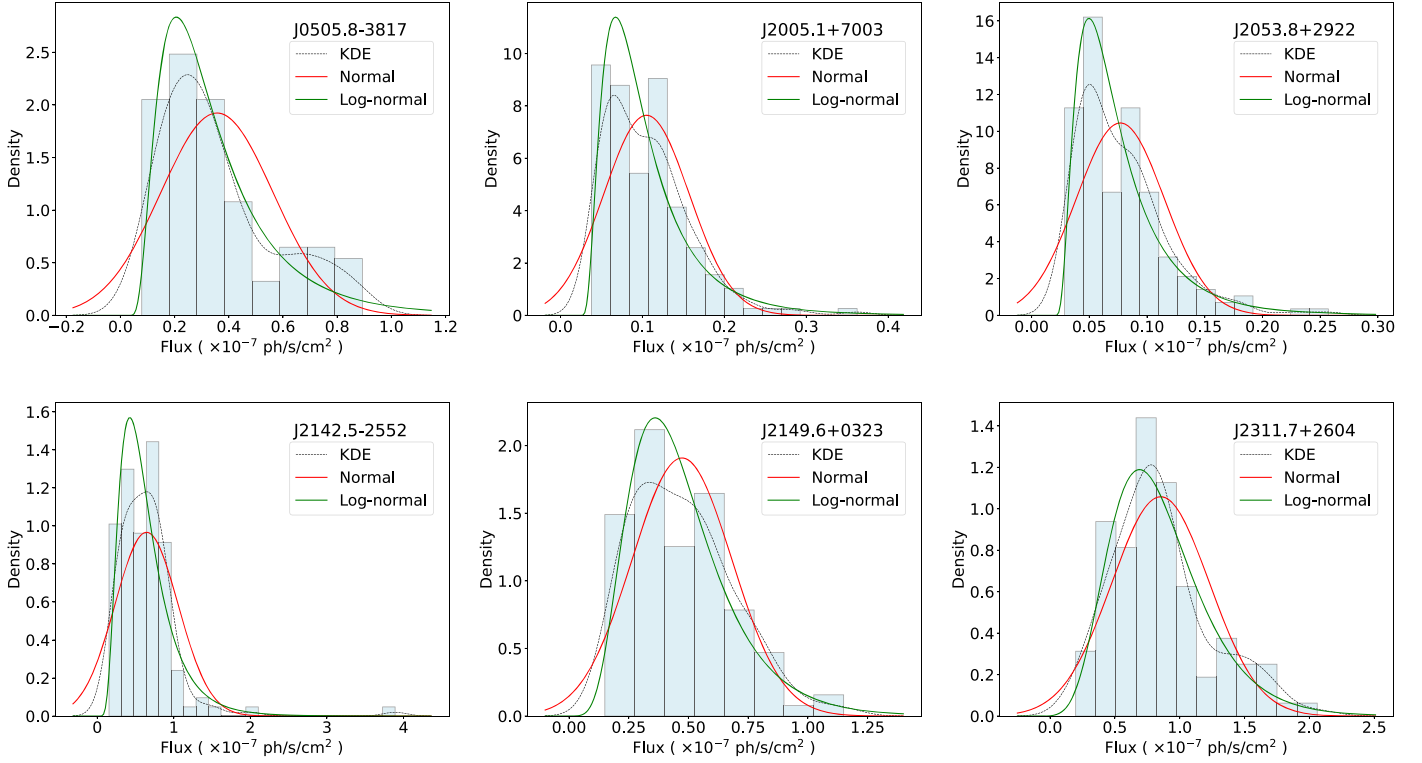
Figure 5. Bimodal of the γ-ray flux distribution (hatched blue), and normal (red) and log-normal (green) PDF fitting to the histogram for the six blazars, the black dotted line represents the kernel density estimation (KDE) curve. Since the statistics is not significant enough, these fits should be taken only as indicative.

Table 4
Statistical Analysis of the Slope and Intercept for the RMS–Flux Relation

		rms $= m*$Flux$+c$			
Points	Mean of m	Mean of c	The Fraction of $m > 0$	The Fraction of $c > 0$	Pearson Correlation
		20 data points			
FSRQs	1.860	-1.190×10^{-8}	100.00%	26.84%	0.977
BL Lacs	1.996	-4.159×10^{-10}	100.00%	29.24%	0.961
BCUs	1.985	-5.483×10^{-8}	100.00%	26.83%	0.979
		40 data points			
FSRQs	2.197	-6.282×10^{-8}	100.00%	22.06%	0.977
BL Lacs	2.417	-3.587×10^{-8}	100.00%	28.39%	0.953
BCUs	2.453	-1.198×10^{-7}	100.00%	24.39%	0.977
		365 days			
FSRQs	2.032	1.232×10^{-7}	100.00%	17.28%	0.981
BL Lacs	2.328	1.128×10^{-8}	100.00%	19.49%	0.970
BCUs	1.966	7.056×10^{-8}	100.00%	17.07%	0.980

explain this behavior (Lyubarskii 1997; Meyer 2019; Khatoon et al. 2020); (2) Inherent particle acceleration in the acceleration region on acceleration timescales leads to linear normal perturbations, which result in log-normal distributions of the flux (Giannios et al. 2009; Narayan & Piran 2012; Sinha et al.

2018); (3) In addition, the log-normal distribution of blazars has also been interpreted as the sum of emission of small jets, i.e., the "minijets in a jet" statistical model (Biteau & Giebels 2012a, 2012b). The "minijets in a jet" model was developed based on the second explanatory model. In the

"minijets in a jet" model, emission from identical, independent but randomly oriented minijets follows the Pareto distribution, which produces both normal and log-normal distributions, while preserving a linear rms–flux relationship in all cases (Biteau & Giebels 2012b). The "minijets in a jet" model is favored by our statistical results: in our blazar sample, in addition to many sources exhibiting log-normal distribution, some other sources also exhibit normal distribution.

In general, the log-normal distribution of the flux implies the linear rms–flux relation (Biteau & Giebels 2012b). Furthermore, the liner rms–flux relation implies that the variability process and the associated perturbations are multiplicative in nature (Lyubarskii 1997; Arévalo & Uttley 2006). Mathematically, the addition process produces a normal distribution, while the multiplication process produces a log-normal distribution. In the X-ray band, the log-normal flux distribution and the linear rms–flux relation can be explained by the accretion disk, inward propagating fluctuations in the disk from different radii accumulate in a multiplicative way (Arévalo & Uttley 2006). Whereas in the γ-ray band, the variability of blazars is primarily associated with the non-thermal radiation from the jet. If the radiation is relativistically beamed, all possible contributing factors, such as such as the variable magnetic field and high-energy particle density, seed-photon density acted upon by the particle acceleration, and diffusion processes could be coupled in a complex manner resulting in the log-normal distribution of flux distribution in blazars(Bhatta & Dhital 2020).

Both normal and log-normal distributions can be interpreted as being special cases of a more general class of skewed distribution, such as Pareto distributions, with variable degrees of skewness. In the Pareto distribution scenario, the resulting flux distribution holds a rms–flux relation (Biteau & Giebels 2012a). We also select the blazars with more than 200 data points for rms–flux fitting of the different types and binnings. The fitting results show that the rms and flux of three subtypes of blazars have a strong linear relationship in three kinds of bins, and their average Pearson coefficient is above 0.95. About 75% of the blazars have an intercept less than 0. Besides, the results show that the slope of BL Lacs was generally greater than that of FSRQs. The strong correlation of the liner rms–flux relation of the blazars belongs to its intrinsic properties. Among the 549 blazars with linear rms–flux relation and the flux distribution of 415, 183, and 187 blazars have lognormality based on the K-S, S-W, and Normality tests, respectively. There are 172 sources are both collected in the 595 source sample and in the 549 source sample. Sources whose flux distribution conforms to the log-normal distribution have a strong linear rms–flux relation. However, the reverse is not true, as the log-normal distribution of flux is not a necessary result of a linear rms–flux relation. The model of "minijets in a jet" indicates that the sample rms is proportional to the sample flux if and only if the flux is the exponential of an underlying variable, as is the case for a log-normally distributed flux. This rms–flux relationship is a necessary and insufficient condition for the log-normal distribution.

References

Abdo, A. A., Ackermann, M., Ajello, M., et al. 2009, ApJS, 183, 46
Abdo, A. A., Ackermann, M., Ajello, M., et al. 2010, ApJL, 725, L73
Abdollahi, S., Acero, F., Ackermann, M., et al. 2020, ApJS, 247, 33
Abdollahi, S., Ajello, M., Baldini, L., et al. 2023, ApJS, 265, 31
Ackermann, M., Ajello, M., Atwood, W., et al. 2015, ApJ, 810, 14
Arévalo, P., & Uttley, P. 2006, MNRAS, 367, 801
Atwood, W. B., Abdo, A. A., Ackermann, M., et al. 2009, ApJ, 697, 1071
Bhatta, G., & Dhital, N. 2020, ApJ, 891, 120
Biteau, J., & Giebels, B. 2012a, in SF2A-2012: Proceedings of the Annual Meeting of the French Society of Astronomy and Astrophysics, ed. S. Boissier et al., 567
Biteau, J., & Giebels, B. 2012b, A&A, 548, A123
Chakraborty, N., Cologna, G., Kastendieck, M. A., et al. 2015, in Proc. of the 34th Int. Cosmic Ray Conf. (ICRC2015) (Trieste: SISSA), 872
Giannios, D., Uzdensky, D. A., & Begelman, M. C. 2009, MNRAS, 395, L29
Giebels, B., & Degrange, B. 2009, A&A, 503, 797
Gleissner, T., Wilms, J., Pottschmidt, K., et al. 2004, A&A, 414, 1091
H.E.S.S. Collaboration, Abdalla, H., Abramowski, A., et al. 2017, arXiv:1709.06442
Jovanović, M. D., Damljanović, G., Taris, F., Gupta, A. C., & Bhatta, G. 2023, MNRAS, 552, 767
Khatoon, R., Shah, Z., Misra, R., & Gogoi, R. 2020, MNRAS, 491, 1934
Kirk, J. G., Rieger, F. M., & Mastichiadis, A. 1998, A&A, 333, 452
Kushwaha, P., Chandra, S., Misra, R., et al. 2016, ApJL, 822, L13
Kushwaha, P., Sinha, A., Misra, R., Singh, K. P., & de Gouveia Dal Pino, E. M. 2017, ApJ, 849, 138
Lyubarskii, Y. E. 1997, MNRAS, 292, 679
Lyutyj, V. M., & Oknyanskij, V. L. 1987, AZh, 64, 465
McClintock, J. E., Narayan, R., Garcia, M. R., et al. 2003, ApJ, 593, 435
McHardy, I. 2010, in Lecture Notes in Physics, Vol. 794 ed. T. Belloni (Berlin: Springer), 203
McHardy, I. M., Uttley, P., Taylor, R. D., & Seymour, N. 2004, in AIP Conf. Ser. 714, X-ray Timing 2003: Rossi and Beyond, ed. P. Kaaret, F. K. Lamb, & J. H. Swank (Melville, NY: AIP), 174
Meyer, M. A. 2019, AGUFM, 33, 1
Narayan, R., & Piran, T. 2012, MNRAS, 420, 604
Peñil, P., Ajello, M., Buson, S., et al. 2022, arXiv:2211.01894
Pottschmidt, K., Wilms, J., Nowak, M. A., et al. 2004, A&A, 411, 383
Quilligan, F., McBreen, B., Hanlon, L., et al. 2002, A&A, 385, 377
Razzano, M., Dumora, D., & Gargano, F. 2009, arXiv:0912.5442
Romoli, C., Chakraborty, N., Dorner, D., Taylor, A. M., & Blank, M. 2018, Galax, 6, 135
Scargle, J. D. 2020, ApJ, 895, 90
Scarpa, R., & Falomo, R. 1997, A&A, 325, 109
Shah, Z., Mankuzhiyil, N., Sinha, A., et al. 2018, RAA, 18, 141
Shah, Z., Misra, R., & Sinha, A. 2020, MNRAS, 496, 3348
Sinha, A., Khatoon, R., Misra, R., et al. 2018, MNRAS, 480, L116
Sinha, A., Sahayanathan, S., Acharya, B., et al. 2017, ApJ, 836, 83
Tluczykont, M., Bernardini, E., Satalecka, K., et al. 2010, A&A, 524, A48
Urry, C. M., & Padovani, P. 1995, PASP, 107, 803
Uttley, P., & McHardy, I. M. 2001, MNRAS, 323, L26
Uttley, P., McHardy, I. M., & Vaughan, S. 2005, MNRAS, 359, 345
Zhang, H., Yan, D., & Zhang, L. 2022, ApJ, 930, 157
Zhang, H., Yan, D., & Zhang, L. 2023, ApJ, 944, 103